Prediction of debris-avalanches and -flows triggered by a tropical storm by using a stochastic approach: An application to the events occurred in Mocoa (Colombia) on 1 April 2017

German Vargas [a], Edoardo Rotigliano [b,*], Christian Conoscenti [b]

[a] Grupo Geotecnologías, Departamento de Geografía, Universidad Nacional de Colombia, Cra. 30 # 45-03, Edificio 212, Bogotá, Colombia

[b] Department of Earth and Marine Sciences (DISTEM), Università degli Studi di Palermo, Via Archirafi 22, 90123 Palermo, Italy

A B S T R A C T

Landslides are among the most dangerous natural processes. Debris avalanches and debris flows in particular have often caused casualties and severe damage to infrastructures in a wide range of environments. The assessment of susceptibility to these phenomena may help policy makers in mitigating the associated risk and thus it has attracted special attention in the last decades.

In this experiment, we assessed susceptibility to debris-avalanche and -flow landslides by using a stochastic approach. Two different modeling techniques were employed: i) Multivariate Adaptive Regression Splines (MARS) and ii) Logistic Regression (LR). Both MARS and LR allow for calculating the probability of landslide occurrence by building statistical relationships between a set of environmental variables and the target variable, i.e. presence/absence of the landslide event. The target variable was extracted from an inventory of debris-avalanche and - flow landslides which were triggered by the tropical storm that hit the area of Mocoa (Colombia) on 1 April 2017. As predictor variables, we employed nine terrain attributes derived from a 5-m resolution DEM (i.e. elevation, slope angle, northness, eastness, upslope slope angle, convergence index, topographic position index, valley depth and topographic wetness index), in addition to lithology, distance from faults and presence/absence of soil creep processes. In our experiment, we used three different landslide datasets which contain i) the highest point of each recognized landslide crown-lines (dataset LIP), ii) the highest 10% of cells of each landslide area (dataset SOURCE), and iii) the entire landslide areas, which include initiation and accumulation zones (dataset MASS). In order to evaluate their predictive ability, LR and MARS models were submitted to *k*-fold spatial cross-validation strategy, which consists in extracting random training and test subsets from *k* spatially disjoint sub-areas. The results of model validation, expressed in terms of Area Under the ROC Curve (*AUC*), demonstrate better predictive performance of MARS models with respect to LR models, for all the three landslide datasets. The mean *AUC* values calculated for the datasets LIP, SOURCE and MASS of the MARS models are 0.776, 0.788 and 0.768, respectively, whereas *AUC* values of the LR models are 0.748, 0.751 and 0.703, respectively. Models validation also show that the predictive skill of the models is better when landslide data are sampled from the highest portions of the landslides (dataset SOURCE). Maps of susceptibility to debris-avalanche and -flow landslides for the Mocoa area were produced by using both LR and MARS and the three landslide datasets. The analysis of the distribution of events versus the susceptibility classes of the maps confirm that MARS and the dataset SOURCE provide the best ability to discriminate between event and non-event cells.

Keywords: Debris flows; Landslide susceptibility; Tropical storm; Multivariate Adaptive Regression Splines (MARS); Logistic Regression (LR); Mocoa (Colombia).

* Corresponding author. Tel.: +39 09123864649; fax: +39 0916169908. E-mail address: edoardo.rotigliano@unipa.it (E. Rotigliano).

1. Introduction

In the last decades, the population growth and the urbanization of hazardous areas have largely increased the damage and loss of lives due to natural disasters. In many developed and developing countries, landslides are among the most important causes of natural hazard (Guzzetti et al., 1999). Landslide hazard is particularly important in mountainous environments where, due to topography, these phenomena may achieve rapid propagation and high energy. Some of the most devastating landslide disasters are related to the occurrence of debris avalanches and debris flows triggered by heavy rainstorms or earthquakes (Hungr et al., 2014). When caused by intense and prolonged rainfalls, these landslides may occur simultaneously with hyperconcentrated flows and flash floods. A dramatic example of their destructive potential is given by the disaster of Vargas (Venezuela) which caused around 15,000 fatalities in December 1999 on a narrow coastal zone north of Caracas (Larsen and Wieczorek, 2006; Larsen, 2008). More recently, in January 2011, over 1,500 casualties were caused by the disaster occurred in the mountainous region of Rio de Janeiro (Brazil), where clusters of debris avalanches and debris flows were triggered by an extreme rainfall event during a period of 2 days (Avelar et al., 2013, Hungr et al., 2014). Other examples of natural disasters that occurred worldwide and related to debris avalanche/flow landslides are reported in the literature (e.g., Crosta and Dal Negro, 2003; Crozier, 2005; Aronica et al., 2012).

Mitigation of landslide risk may be achieved by predicting where landslides are more likely to occur in the future. This information could indeed help policy-makers in implementing land-use strategies aimed at minimizing human casualties and property damage (Guzzetti et al., 1999). The likelihood of landslide occurrence in a given area is defined as landslide susceptibility (Brabb, 1984; Carrara et al., 1995). A landslide susceptibility map depicts the spatial relative probability of landslide occurrence within a given area (Conoscenti et al., 2016).

Landslide susceptibility mapping can be achieved by using different methods. Among them, the stochastic approach has become very popular over the last decades, due to the availability of high-resolution terrain data and freeware statistical and Geographical Information Systems (GIS) software. This approach is based on the assumption that “the past is the key to the future” (Carrara et al., 1995) and new slope failures are more likely to occur under the same conditions that caused landsliding in the past. Therefore, statistical methods require the location of past landslides and maps of environmental variables which directly or indirectly (as proxies) reflect the preparatory factors controlling landslide occurrence in the study area. Different statistical and data mining modeling techniques have been proved to provide reliable and accurate landslide susceptibility maps starting from event inventories and sets of predictor variables (Aleotti and Chowdhury, 1999; Guzzetti et al., 1999; Brenning, 2005; Reichenbach et al., 2018).

Although widely adopted in recent years, statistical modeling of landslide susceptibility involves some critical issues which still remain unsolved. One of these is related to the selection of event and non-event data which are employed to calibrate and validate the landslide predictive models. This is recognized as a crucial step influencing the accuracy and reliability of the final landslide susceptibility models and maps.

In case of grid-based landslide predictions, non-event locations are typically sampled from stable portions of slopes, i.e. cells outside the landslide areas. On the other hand, no agreement exists on the best approach to select landslide cells. These should identify landscape locations where levels of the landslide controlling factors exceeded the threshold of slope stability and, thus, triggered the slope failure. However, identifying the exact initiation points of a large number of landslides is very problematic (Regmi et al., 2014). In the case of debris avalanches or flows, even distinguishing between source and accumulation zones could be quite difficult. Furthermore, once initiated, a landslide can extend upslope, downslope and/or sidewise, making the identification of the initiation point a very challenging task.

Various landslide data selection and sampling techniques have been proposed to minimize the uncertainty in identifying landslide initiation points. The most frequently adopted strategies are: i) single cells randomly selected from landslide areas or from depletion zones (e.g., Vorpahl et al., 2012; Heckmann et al., 2014; Goetz et al., 2015); ii) centroid of landslide areas or of depletion zones (e.g., Atkinson and Massari, 2011; Regmi et al., 2014); iii) multiple cells (all or a fraction) within landslide areas or depletion zones (e.g., Regmi et al., 2014; Conoscenti et al., 2016); iv) single cell or all the cells in the upper edge of the main scarp (e.g., Clerici et al., 2006; Costanzo et al., 2012; Cama et al., 2015; 2017). Moreover, when the available DEM is more recent than the landslide inventory, topographic triggering conditions are sampled from a buffer around the landslide polygons (e.g., Süzen and Doyuran, 2004; Nefeslioglu et al. 2008; Rotigliano et al., 2011) or from a reconstructed pre-failure topography within landslide areas (e.g., Van Den Eeckhaut et al. 2006; Gorum et al. 2008; Conoscenti et al., 2015).

Intense and prolonged rainfall events occur episodically in tropical Andes, triggering debris-avalanche and -flow landslides, hyperconcentrated flows and flash floods. These natural hazards threaten many communities living on or near alluvial fans where they may cause fatal victims and extensive property damage. The assessment of susceptibility to debris-avalanche and -flow landslides in these environments is therefore crucial to plan risk mitigation strategies and prevent large disasters.

On 1 April 2017, the area of Mocoa (Colombia) was hit by a sever tropical storm which discharged 130 mm of rain in 3 h starting from 10:00 pm of March, 31st. This heavy rainfall triggered more than one thousand debris-avalanche and -flow landslides, which evolved to hyperconcentrated flows in the main streams of the Mulato, Sangoyaco and Taruca rivers, three tributaries of the Mocoa river. The event caused 328 victims, 200 missing, more than 1000 injured and damage to more than 120 houses in 17 neighborhoods of the city.

In this study we focused on the prediction of the rainfall-induced debris-avalanche and -flow landslides which occurred in the area of Mocoa. These processes initiated on the slopes and provided sediments to hyperconcentrated flows which moved rapidly down steep channels and caused debris flooding of large parts of the city located on the alluvial fans. Within the context of testing different methods of landslide data sampling for susceptibility modeling, we used and compared three criteria which differ in the way the event data were selected. The landslide datasets employed in our experiment include (i) the highest point of each landslide area, (ii) the highest 10% of cells of the landslide areas or (iii) the entire landslide areas. To predict the spatial distribution of the Mocoa landslides, we used two different statistical modeling techniques, namely: (i) logistic regression (LR) and (ii) multivariate adaptive regression splines (MARS). LR has been widely adopted to assess landslide susceptibility and, in particular, debris avalanche/flow landslides. Conversely, MARS has been rarely used in the field of landslide susceptibility mapping and, as far as we know, has been employed to predict these types of slope failures only in one research study (Rotigliano et al., 2018).

Therefore, the main objectives of this experiment were to: (i) test and compare three different criteria of landslide data sampling; (ii) evaluate and compare the ability of LR and MARS to predict the debris-avalanche and -flow landslides occurred in Mocoa.

2. Study area

The study area is located in the southeast portion of the Eastern Cordillera of the Colombian Andes and falls in the watershed of the Mocoa River (Fig. 1). It extends for 58.3 km^2 and lies between latitudes 01° 08’ and 01° 13’ N and longitudes 76° 38’ and 76° 42’ W. The city of Mocoa, capital of the Departamento de Putumayo, is located in the southeast sector of the study area. Its urban area is bounded to the east by the Mocoa river and is crossed by three of its tributaries: Taruca, Sangoyaco and Mulato. Precipitation in the study area occurs all year long and shows a unimodal annual pattern with highest and lowest average monthly rainfall occurring in June and January, respectively. The average annual rainfall is approximately 3715 mm.

The topography of the study area varies from flat to hilly to steep, with elevation ranging from 538 to 1893 m asl (Figs. 2 and 3). The western portion is characterized by moderately dissected mountain chains with very steep slopes (up to 77°). These are followed to the east by a hilly sector where topography is mainly controlled by structure and the slope angle is in the range 10–25°. Gentle-sloping (<10°) surfaces, which are formed by coalescing debris fans, occur on the right Mocoa riverside. A structure-controlled relief, which is located to the north of the Mocoa urban area, acts as a natural barrier to protect the city from flooding events. Moreover, flat surface (i.e. river terraces and alluvial plains) are located along the inter-mountainous sector of the Mocoa river. The study area is underlain by Jurassic igneous rocks and Cretaceous and Paleocene-Eocene sedimentary rocks, which are covered discordantly by Quaternary unconsolidated deposits. To explore the role of lithology as a predictor of landslide distribution, we prepared a map that includes the following lithological units: i) sedimentary rocks, mainly conglomerates; ii) sedimentary rocks, mainly calcareous limestones; iii) igneous rocks mainly granites and monzonites; iv) alluvial deposits; v) terraced alluvial deposits; vi) colluvial deposits; vii) debris-torrent deposits (Fig. 4). The igneous rocks, which are moderately to highly fractured, crop out in the western sector of the study area. The La Tebaida fault separates these rocks to the east from the Paleocene-Eocene conglomerates of the Pepino Fm., whereas the limestones of the Villeta Fm. outcrop in the eastern side of the Mocoa River. The quaternary deposits occupy the Mocoa river bed and form fluvial terraces along its main valley. Moreover debris fans occur along the Mocoa tributaries while colluvial deposits cover the foot of some slopes along the inter-mountain valleys.

3. Materials and methods

3.1. Landslide inventory

The rainfall event considered in this study occurred between 10 pm of March, 31st and 1 am of April, 1st, 2017. The event was short but very intense with 130 mm of rain that fell in about 3 h. Such an amount of rain usually occurs in a ten days time-lapse. The rainfall event triggered a high number of debris avalanches and debris flows which propagated downslope as hyperconcentrated flows and debris floods.

The landslides occurred in the slopes that fed the streams of the Taruca, Sangoyaco and Mulatos rivers with a large amount of debris and blocks (with diameter up to six meters). These sediments were transported downslope and covered an area of approximately 3.2 km^2, with average thickness of 4 m and a total volume of around 12 millions of cubic meters.

In this work, we built a landslide inventory by 2D and 3D visual analysis of aerial photographs and of the satellite image dated April 10th, 2017, available on Google Earth. The inventory includes 1347 landslides (Fig. 5). Based on Hungr et al. (2014), two main types of movements were recognized: i) debris avalanches, which occurred on steep slopes and without confinement in an established channel and ii) debris flows, in which the movement developed along established paths, usually first or second order streams.

The mapped slope failures probably initiated as shallow slides or flows (Cruden and Varnes, 1996) and after moving a short distance transformed into debris avalanches or debris flows. However, considering that the objective of this experiment was to identify where slope failures potentially reaching the drainage axes and, eventually, the urbanized area of Mocoa, were more likely to occur, we decided not to differentiate between the two types of movements in the susceptibility mapping.

3.2. Predictor variables

In this experiment, selection of landslide predictors was performed according to quality and resolution of the available data. As spatial distribution of the rainfall event was not available, only variables representing landslide preparatory causes were employed.

The landslide predictors were derived from a geological map of the area and a 5-m resolution raster Digital Elevation Model (DEM), which provided sufficient resolution to properly map susceptibility to landsliding in the Mocoa area. Conversely, the resolution of existing land cover and soil maps were too coarse and thus not suitable for the analysis. All the variables were prepared as raster GIS layers with 5-m cell size. The following predictors were derived from the DEM using SAGA-GIS software (Conrad et al., 2015): elevation (*ELEV*), slope angle (*SLOPE*), northness (*NORTH*), eastness (*EAST*), upslope slope angle (*UPSLO*), convergence index (*CONV*), topographic position index (*TPI*), valley depth (*VDEP*) and topographic wetness index (*TWI*). These attributes were selected as proxies for conditions and processes related to landslide occurrence (e.g., Wilson and Gallant, 2000; Ohlmacher, 2007; Vorpahl et al., 2012). *ELEV* reflects the values of the available 5-m DEM and was selected because of its expected correlation with rainfall and vegetation spatial distribution. *SLOPE* was calculated according to Zevenbergen and Thorne (1987). *NORTH* and *EAST* were computed by applying cosine and sine transformations of slope aspect, respectively (Brenning and Trombotto, 2006; Conoscenti et al., 2016; Cama et al., 2017). *NORTH*, *EAST*, as well as *ELEV*, may serve as proxies for seasonal wet/dry cycles of soils (Auslander et al., 2003). *UPSLO* reflects average slope angle upstream from each position in the landscape. *CONV* (Koethe and Lehmeier, 1996), which estimates to what extent neighboring cells point to the center cell, was calculated by setting a search radius of 50-m. To reduce detail and remove noise of the *TWI* (Beven and Kirkby, 1979), a gaussian smoothing filter with search radius of 25-m was applied. *CONV* and *TWI* were included to account for runoff convergence/divergence and potential soil saturation, respectively. *TPI* (Guisan et al., 1999) indicates the relative position of each cell and was calculated by using a 100-m search radius. *TPI* and *CONV* values are negative on valley bottoms and positive on ridges. *VDEP* reflects the maximum relative relief measured in cross-sections and thus is a measure of local relief energy (Lóczy et al., 2012).

Moreover, we employed lithology (*LITHO*), distance form faults (*FAULTD*) and presence/absence of soil creep (*CREEP*) as predictor variables. *LITHO* was prepared by grouping the geological formations that outcrop in the study area into 7 geological units, according to their expected relationship with slope stability (Fig. 4). *FAULTD* was included to potentially reflect the degree of weakening of the bedrock due to tectonically active regional geological structures (Mathew et al., 2009; Cama et al., 2017). *CREEP* includes 71 areas (extending between 1 and 285 ha) affected by soil creep (Fig. 5), which in the region is favored by deforestation for agriculture and pasture. *CREEP* was prepared by analyzing the same images employed to map the landslides.

3.3. Statistical modeling

Probability of debris-avalanche and -flow landslide occurrence at each 5-m grid cell in the study area was calculated by employing two statistical modeling techniques: logistic regression (LR; Hosmer and Lemeshow, 2000) and multivariate adaptive regression splines (MARS; Friedman, 1991). The statistical analyses were performed using the R software (R Core Team, 2017) with the packages “usdm” (Naimi, 2015), “sperrorest” (Brenning, 2012) and “earth” (Milborrow et al., 2015).

LR is among the most frequently used statistical technique for spatial modeling of landslide occurrence (Brenning, 2005) and it has been employed several times to predict specifically storm-triggered landslides (e.g., Chevalier et al., 2013; Heckmann et al., 2014; Lombardo et al., 2014, 2015; Cama et al., 2016; Trigila et al., 2015). On the other hand, MARS has been employed only rarely for assessing landslide susceptibility (e.g., Vorpahl et al., 2012; Felicísimo et al., 2013; Conoscenti et al., 2015, 2016; Pourghasemi and Rossi, 2016) and, as far as we know, this modeling technique was exploited for predicting landslides triggered by extreme rainfall events only in one recent research paper (Rotigliano et al., 2018). LR and MARS can use both continuous and categorical independent variables to estimate a response variable in the range 0 to 1, which can be interpreted as probability of an event occurrence. Both LR and MARS consist of an additive combination of terms. Each term of the LR model is given by a linear regression of an independent variable, which is fitted using the maximum likelihood method. In contrast to the assumption of LR that coefficients of the predictors are constant across their ranges, MARS splits the range of the independent variables into pieces, fitting to each of them a linear regression called “basis function” (Vorpahl et al., 2012; Gómez-Gutiérrez et al., 2015; Conoscenti et al., 2018; Garosi et al., 2018). MARS terms consist of a single basis function or a product of two or more of them. To reduce the complexity of the LR models and avoid problems of overfitting, we adopted a bilateral stepwise strategy that selects only the most significant predictors. Accordingly, MARS models were prepared by avoiding terms consisting of more than one basis function.

As both LR and MARS require the absence of multicollinearity (i.e. predictors should not be correlated with each other), we calculated the variance inflation factor (*VIF*) to measure the degree of correlation among the selected predictors. The R package “usdm” was employed to this aim. Following the “rule of 10”, according to which a $VIF > 10$ reveals strong multicollinearity

(Heckmann et al., 2014; Jebur et al., 2014; Bui et al., 2015), we decided to include in the models all the above cited variables, as their *VIF* values are well below the threshold.

3.4. Landslide data sampling

In our experiment we used three different methods to select landslide data (Fig. 6). The three methods differ in the way event cells were selected. A single approach was instead employed to pick up non-event cells. These were randomly sampled from stable portions of the slopes, i.e. cells outside landslide areas (dataset STABLE). Landslide data samples were always prepared by maintaining a presence-absence ratio of 1:1. This choice was made in order to avoid prevalence in the samples (i.e. different proportion of event and non-event observations), which has been shown to affect the reliability of common accuracy statistics (Beguería, 2006).

In the first approach we selected a single cell at the highest point of each of the recognized landslide crown-lines (hereafter named LIP; Lombardo et al., 2015; Cama et al., 2015, 2016), identifying a total of 1347 event cells (dataset LIP). As model performance and robustness can be affected by the size of calibration and validation datasets (Brenning, 2005; Vorpahl et al., 2012), the same number of event cells was selected also using the other two methods. In our second approach, event cells were randomly sampled from the upper portions of the mapped landslides, which should reflect the conditions of the main source areas. These portions include the highest 10% of cells of each landslide area (dataset SOURCE). In the third method, landslide cells were randomly picked up from the entire landslide areas, which include initiation and accumulation zones (dataset MASS). In the second and third approach, we sampled as event cells a relative small fraction of pixels within both upper portions (around 12% of 11,294 cells) and entire landslide areas (around 1.2% of 109,149 cells). In this way, we limited the effects of spatial autocorrelation between sampled cells, which should be avoided when performing statistical prediction of landslide occurrence.

3.5. Models training and validation strategy

In order to evaluate their predictive ability, LR and MARS models were submitted to a *k*-fold spatial cross-validation strategy, which consists in extracting random training and test subsets from *k* spatially disjoint sub-areas. These were identified by using the *k*-means clustering algorithm (Ruß and Brenning, 2010; Goetz et al., 2015). As classic *k*-fold cross validation, the adopted approach uses k - 1 combined subsets at time for calibration and the remaining one for validation. The process is then repeated *k* times.

In our experiment we used $k = 5$ spatial cross-validation folds. To improve the robustness of the landslide predictions and mitigate the rare-events issue (Heckmann et al., 2014; Svoray et al., 2012; Van Den Eeckhaut et al., 2012), multiple learning samples were extracted for each fold. More in detail, our approach included the following steps, which were repeated for each of the five folds: i) sampling of ten balanced subsets from the four (i.e. k - 1) calibration sub-areas; ii) training a model on each of the ten calibration subsets; iii) sampling of a balanced subset from the validation sub-area; iv) calculating a probability (*P*) of landslide occurrence in the validation subset by averaging the scores obtained from the ten model runs; v) estimation of the model performance by averaging the performance evaluated across each of the five folds. To assess the robustness of our approach, this validation process was repeated 100 times for both LR and MARS models.

The prediction skill of the models was evaluated with the area under the receiver operating characteristics (ROC) curve (*AUC*). The ROC curve plots for all possible cut-off values the true positive rate *TPR* (sensitivity) versus the false positive rate *FPR* (1 – specificity). *AUC* values close to 1 indicate perfect discrimination ability between the target variable levels (0 or 1) whereas values close to 0.5 reflect no discrimination ability of the models. Intermediate *AUC* values were interpreted as acceptable, excellent or outstanding if higher than 0.7, 0.8 and 0.9, respectively (Hosmer and Lemeshow, 2000). The Wilcoxon signed-rank test was applied to detect significant differences in model performance. Differences at p-value < 0.01 were considered significant.

3.6. Debris-avalanche and -flow landslide susceptibility maps

A total of six debris-avalanche and -flow landslide susceptibility maps were prepared for the area of Mocoa by using LR and MARS with samples extracted from the datasets LIP, SOURCE and MASS. The following procedure was applied for both the modeling techniques (i.e. LR and MARS) and the three datasets (i.e. LIP, SOURCE and MASS): i) sampling of 100 balanced subsets made of 2694 cells; ii) calibration of a model for each of the 100 subsets of cells; iii) calculation of probability (P) of landslide occurrence for each cell of the study area by averaging the scores obtained from the 100 model runs. The range of debris avalanche/flow probability (0.00 – 1.00) was classified into four equal interval levels (interval width: 0.25). As both LR and MARS models were prepared using balanced datasets of event and non-event pixels, the score averaged from the 100 model runs should be interpreted as relative probability of debris avalanche/flow occurrence (Goetz et al., 2015).

4. Results

4.1. Validation of the susceptibility models

The predictive performance of LR and MARS evaluated for the three datasets is summarized in Fig. 7 by using six box plots. Each box plot shows the variability of 100 AUC values which were computed by means of the validation procedure described in Section 3.5. The average AUC values of LR and MARS calculated for the three datasets are all in the range 0.7 – 0.8, demonstrating an acceptable ($AUC > 0.7$) overall accuracy of the debris-avalanche and -flow landslide predictive models in the area of Mocoa. However, significant differences are revealed if we compare the performance of the models by applying the Wilcoxon signed-rank test.

The 100 MARS model runs validated on the dataset SOURCE (mean $AUC = 0.788$) demonstrated a significant (p-value < $2.2e^{-16}$) higher accuracy than those tested on the dataset LIP (mean AUC = 0.776), which in turns performed better (p-value = $7.23e^{-07}$) than the MARS-MASS model runs (mean AUC = 0.768). On the other hand, no significant (p-value = 0.1355) difference of performance was measured between LR predictions of LIP (mean *AUC* = 0.748) and SOURCE (mean *AUC* = 0.750) datasets whereas LR-MASS model runs clearly exhibited the poorest predictive performance (mean *AUC* = 0.703). In all three datasets, MARS runs outperformed LR model repetitions (p-value < $2.2e^{-16}$).

As regards performance variation, which was evaluated by means of the standard deviation (SD), MARS- and LR-LIP models exhibited very similar robustness (SD: 0.0075 vs 0.0076), whereas MARS predictive skill was slightly more stable when validated on the SOURCE (SD: 0.0098 vs 0.0117) and MASS datasets (SD: 0.0102 vs 0.0131). For any of the two modeling techniques, *AUC* values dispersion increases from LIP, through SOURCE to MASS datasets.

4.2. MARS and LR susceptibility maps

The six debris-avalanche and -flow landslide susceptibility maps prepared with MARS and LR using the three landslide datasets are plotted in Fig. 8. To help compare and evaluate the maps, Fig. 9 shows the relative frequency distributions of the datasets ALL (all pixels in the study area), STABLE, LIP, SOURCE and MASS over the four relative probability classes, for each of the six maps.

All the maps show smooth prediction patterns without abrupt changes where boundaries of categorical variables (i.e., lithology and soil creep presence/absence) occur.

MARS provides for all landslide datasets a smoother distribution of the susceptibility classes over the entire maps (dataset ALL), with a gradually decreasing frequency from the lowest to the highest class of landslide probability (P). Conversely, except for the SOURCE map, LR produces roughly similar frequency of P classes between 0.00 and 0.75 whereas the highest class occurs more rarely.

Non-event pixels (dataset STABLE) are better discriminated by the MARS-SOURCE map, where 75% of the stable points has a low susceptibility level (i.e. $P < 0.5$) whereas only 67% has a P value below 0.5 in the LR-LIP map.

Fig. 9 shows that, if we consider $P = 0.5$ as threshold to discriminate between pixels predicted as stable ($P < 0.5$) and unstable ($P > 0.5$), event cells of the datasets LIP, SOURCE and MASS are predicted with excellent sensitivity (or true positive rate, TPR) by both MARS (TPR range: 0.77 – 0.78) and LR (TPR range: 0.76 – 0.78) maps. However, if we focus on the distribution of event pixels with P > 0.5, Fig. 9 reveals that, except for LIP maps, they are roughly equally distributed between the two highest levels of susceptibility in the MARS maps, whereas event pixels are less frequent in the highest *P* class of LR maps.

5. Discussion

The spatial cross-validation revealed that the statistical predictive models provided an acceptable fit to the spatial distribution of the landslides occurred in the study area during the night between March 31 and April 1, 2017. Although MARS and LR models provided apparently comparable ability to discriminate between event and non-event pixels on the three landslide datasets (i.e. LIP, SOURCE, MASS), the Wilcoxon signed-rank test revealed significant differences of performance. MARS models, indeed, showed a better prediction skill in all landslide datasets, with a mean *AUC* difference of 0.044.

The existence of non-linear relationships between selected predictors and slope failures in the study area can explain the better fit of MARS models to the landslide datasets. LR models are indeed based on linear relationships holding over the entire range of the explanatory variables whereas MARS is able to split the range of predictors into pieces and fit to each of them a different linear regression. In this way, MARS produces a smooth response curve which may better reproduce the relationships between predictors and landslide occurrence.

The better performance of MARS in our study area is consistent with the findings of few other previous works that compared the ability of LR and MARS in predicting landslide occurrence. A similar difference of mean *AUC* values between LR and MARS (0.848 against 0.889) was found by Conoscenti et al. (2015) in a catchment of Sicily (Italy) affected by earth-flow landslides. Roughly the same difference of prediction skill was revealed by internal cross validation that was applied to an inventory of shallow translational landslides in the Andes of Southern Ecuador (Vorpahl et al., 2012). A slightly better performance of MARS (*AUC* = 0.782) with respect to LR (*AUC* = 0.775) was found by Pourghasemi and Rossi (2016), who compared the ability of four statistical techniques to predict landslides occurred in the Mazandarn Province (Iran). On the other hand, LR and MARS achieved the same accuracy (AUC = 0.76) in predicting the landslide spatial distribution in Guipúzcoa province (Spain; Felicísimo et al., 2013). Also, Vorpahl et al. (2012) found no significant difference of predictive performance when they applied an external cross validation to their data.

The results of our experiment and those of the above cited papers suggest that the role of a physical factor in controlling a geomorphological process can be better represented by a series of local functions rather than a single linear regression. In other words, simple predictive models, which are typically employed to explain relationships between factors and geomorphological processes, are less accurate than complex models, such as those provided by MARS.

As regards the different landslide datasets employed in this experiment, we found a significant lower accuracy when predictive models were calibrated and validated using event pixels sampled from the entire landslide areas (i.e. dataset MASS). The best fit to landslide data was found when we used MARS with event cells sampled from the highest 10% of cells of each landslide area (dataset SOURCE) whereas no significant difference of performance was detected when we trained and tested LR models with datasets LIP and SOURCE.

The overall better discrimination ability of the LIP/SOURCE pixels can be explained considering that their terrain conditions are more specific than those of the MASS cells. The latter indeed may occur on the initiation, transport and deposition zones of debris-avalanches and -flows which can be characterized by heterogeneous conditions (e.g., altitude, slope, convergence index, TPI, TWI or valley depth) within each individual landslide area, whereas LIP/SOURCE pixels should likely have more homogeneous conditions. These results are consistent with those of Regmi et al. (2014), who found that accuracy of landslide predictive models was slightly better when developed on samples obtained from scarps of different types of landslides (i.e., debris flows, debris slides, rock slides and soil slides) occurred in western Colorado, USA. They explain their findings assuming that landslides in their study area were mainly due to unfavorable condition at the slope heads and, thus, data sampling from scarps instead of landslide masses reduced uncertainties. On the other hand, Vorpahl et al. (2012) found better performance in predicting landslide deposition zones than initiation zones. As possible reason of this result, they assumed that deposition zones mainly occur close to bottom of small valleys which can be described by the selected terrain attributes better than the open slope where initiation zones tend to be located. In other words, also Vorpahl et al. (2012) assume that more specific terrain conditions of landslide data provide more accurate predictive skill of the models.

Although apparently similar, the six debris-avalanche and -flow landslide susceptibility maps obtained from MARS and LR models have important differences, which are revealed by the histograms of Fig. 9. Based on the latter, we can infer that, also across the entire study area, MARS performed better than LR and both modeling techniques achieved better prediction skill when employed to discriminate between stable and unstable pixels of the dataset SOURCE. We consider MARS maps better than LR maps because of the following reasons. First, frequency of susceptibility levels of MARS maps gradually decreases from lowest to highest ones, which is a desirable quality for landslide susceptibility maps. Indeed, as landsliding is normally a rare-event and thus ratio of event to non-event cells can be very low, maps with high frequency of susceptible pixels can suffer from high false positive rates. Second, using $P < 0.5$ as threshold to identify non-susceptible pixels, MARS maps are characterized by significantly higher specificity (or true negative rate) on all analyzed landslide datasets. Third, MARS maps have higher percentage of event pixels with $P > 0.75$. Similarly, it is reasonable to infer that dataset SOURCE yielded better MARS and LR maps because, although roughly the same true positive rate (P threshold = 0.5) was observed for all landslide datasets, the percentage of event pixels with $P > 0.75$ was definitely higher. Furthermore, a higher percentage of stable pixels with $P < 0.5$ occur in MARS- and LR-SOURCE maps.

The results of this experiment demonstrated that a stochastic approach can be used by geomorphologists to achieve reliable prediction of landslides triggered by an extreme rainfall event in a mountainous environment. The approach described in this paper could be useful particularly in developing countries which have great difficulty in affording the high costs of structural measures to reduce landslide risk. This method allows for identifying areas prone to landsliding and thus could provide a valuable aid to a rational land use planning aimed at minimizing victims and economic damage.

6. Concluding remarks

In this experiment, we employed a stochastic approach to predict the spatial distribution of the debris-avalanches and -flows triggered by heavy rainfalls occurred in the area of Mocoa on April 1st, 2017. Multivariate Adaptive Regression Splines (MARS) and Logistic Regression (LR) were exploited as modeling techniques. A set of nine terrain attributes, in addition to lithology, distance from faults and presence/absence of soil creep processes were used as predictor variables. Validation of the models was performed by using *k*-fold spatial cross-validation and by calculating *AUC* values of 100 MARS and LR model repetitions applied to balanced samples of event and non-event pixels. The calibration and validation samples were extracted from three different landslide datasets which contain the highest point of each landslide crown-line (dataset LIP), the highest 10% of cells of each landslide area (dataset SOURCE) or the entire landslide area (dataset MASS).

The following conclusions can be drawn for the Mocoa study area on the basis of the validation of the models and the analysis of six susceptibility maps which were obtained by using MARS and LR with the three landslide datasets.

1. The overall accuracy of our models can be considered acceptable ($AUC > 0.7$);
2. MARS models and maps exhibited a better ability to discriminate between event and non-event pixels;

3. Both MARS and LR demonstrated better accuracy when employed to predict landslide source areas;
4. The relationships between predictors and debris-avalanche and -flow landslides are more accurately reproduced by piecewise linear regressions rather than individual linear functions holding over the entire predictor range.

The approach employed in this experiment is relatively simple, rapid and can be reproduced by using free software and data usually available. It can be used to prepare debris-avalanche and -flow landslide susceptibility maps which can help policy makers and land managers of Colombia to establish preventive measures and mitigate risks.

Acknowledgements

The research was supported by the following projects: i) CoRI project-2017 awarded to Christian Conoscenti and funded by the Università degli Studi di Palermo; ii) Project titled “Geología y Geomorfología de ríos tropicales. Conocer los ríos previene desastres" (codigo 41500) awarded to German Vargas and funded by the Universidad Nacional de Colombia. All the authors have commonly shared the whole research phases. This manuscript benefited greatly from the kind suggestions and comments of Prof. Takashi Oguchi, Prof. Allen Bateman and one anonymous reviewer.

References

Aleotti, P., Chowdhury, R., 1999. Landslide hazard assessment: summary review and new perspectives. Bull. Eng. Geol. Environ. 58, 21–44. doi:10.1007/s100640050066

Aronica, G.T., Brigandí, G., Morey, N., 2012. Flash floods and debris flow in the city area of Messina, north-east part of Sicily, Italy in October 2009: The case of the Giampilieri catchment. Nat. Hazards Earth Syst. Sci. 12, 1295–1309. doi:10.5194/nhess-12-1295-2012

Atkinson, P.M., Massari, R., 2011. Autologistic modelling of susceptibility to landsliding in the Central Apennines, Italy. Geomorphology 130, 55–64. doi:10.1016/j.geomorph.2011.02.001

Auslander, M., Nevo, E., Inbar, M., 2003. The effects of slope orientation on plant growth, developmental instability and susceptibility to herbivores. J. Arid Environ. 55, 405–416. doi:10.1016/S0140-1963(02)00281-1

Avelar, A.S., Netto, A.L.C., Lacerda, W.A., Becker, L.B., Mendonça, M.B., 2013. Mechanisms of the Recent Catastrophic Landslides in the Mountainous Range of Rio de Janeiro, Brazil BT - Landslide Science and Practice: Volume 4: Global Environmental Change, in: Margottini, C., Canuti, P., Sassa, K. (Eds.), Springer Berlin Heidelberg, Berlin, Heidelberg, pp. 265–270. doi:10.1007/978-3-642-31337-0_34

Beguería, S., 2006. Validation and Evaluation of Predictive Models in Hazard Assessment and Risk Management. Nat. Hazards 37, 315–329. doi:10.1007/s11069-005-5182-6

Beven, K.J., Kirkby, M.J., 1979. A physically based variable contributing area model of basin hydrology. Hydrol. Sci. Bull. 24, 43–69. doi:http://dx.doi.org/10.1080/02626667909491834

Brabb, E.E., 1984. Innovative approaches to landslide hazard and risk mapping, in: Proceedings 4th International Symposium on Landslides Vol. 1. Toronto, Canada, pp. 307–324.

Brenning, A., 2005. Spatial prediction models for landslide hazards: review, comparison and evaluation. Nat. Hazards Earth Syst. Sci. 5, 853–862. doi:10.5194/nhess-5-853-2005

Brenning, A., Trombotto, D., 2006. Logistic regression modeling of rock glacier and glacier distribution: Topographic and climatic controls in the semi-arid Andes. Geomorphology. doi:10.1016/j.geomorph.2006.04.003

Brenning, A., 2012. Improved spatial analysis and prediction of landslide susceptibility: Practical recommendations. Landslides Eng. Slopes Prot. Soc. through Improv. Understanding, Proc. 11th Int. 2nd North Am. Symp. Landslides Eng. Slopes, Banff, Canada 789–794.

Bui, D.T., Tuan, T.A., Klempe, H., Pradhan, B., Revhaug, I., 2015. Spatial prediction models for shallow landslide hazards : a comparative assessment of the efficacy of support vector machines , artificial neural networks , kernel logistic regression , and logistic model tree. Landslides. doi:10.1007/s10346-015-0557-6

Cama, M., Lombardo, L., Conoscenti, C., Rotigliano, E., 2017. Improving transferability strategies for debris flow susceptibility assessment: Application to the Saponara and Itala catchments (Messina, Italy). Geomorphology 288, 52–65. doi:10.1016/j.geomorph.2017.03.025

Cama, M., Conoscenti, C., Lombardo, L., Rotigliano, E., 2016. Exploring relationships between grid cell size and accuracy for debris-flow susceptibility models: a test in the Giampilieri catchment (Sicily, Italy). Environ. Earth Sci. 75. doi:10.1007/s12665-015-5047-6

Carrara, A., Cardinali, M., Guzzetti, F., Reichenbach, P., 1995. GIS technology in mapping landslide hazard, in: Carrara, A., Guzzetti, F. (Eds.), Geographical Information Systems in Assessing Natural Hazards. Kluwer, Dordrecht, pp. 135–175.

Chevalier, G.G., Medina, V., Hürlimann, M., Bateman, A., 2013. Debris-flow susceptibility analysis using fluvio-morphological parameters and data mining : Nat. Hazards 67, 213–238. doi:10.1007/s11069-013-0568-3

Clerici, A., Perego, S., Tellini, C., Vescovi, P., 2006. A GIS-based automated procedure for landslide susceptibility mapping by the Conditional Analysis method: the Baganza valley case study (Italian Northern Apennines). Environ. Geol. 50, 941–961. doi:10.1007/s00254-006-0264-7

Conoscenti, C., Agnesi, V., Cama, M., Caraballo-Arias, N.A., Rotigliano, E., 2018. Assessment of Gully Erosion Susceptibility Using Multivariate Adaptive Regression Splines and Accounting for Terrain Connectivity. L. Degrad. Dev. 29, 724–736. doi:10.1002/ldr.2772

Conoscenti, C., Ciaccio, M., Caraballo-Arias, N.A., Gómez-Gutiérrez, Á., Rotigliano, E., Agnesi, V., 2015. Assessment of susceptibility to earth-flow landslide using logistic regression and multivariate adaptive regression splines: A case of the Belice River basin (western Sicily, Italy). Geomorphology 242, 49–64. doi:10.1016/j.geomorph.2014.09.020

Conoscenti, C., Rotigliano, E., Cama, M., Caraballo-Arias, N.A., Lombardo, L., Agnesi, V., 2016. Exploring the effect of absence selection on landslide susceptibility models: A case study in Sicily, Italy. Geomorphology 261, 222–235. doi:10.1016/j.geomorph.2016.03.006

Conrad, O., Bechtel, B., Bock, M., Dietrich, H., Fischer, E., Gerlitz, L., Wehberg, J., Wichmann, V., Böhner, J., 2015. System for Automated Geoscientific Analyses (SAGA) v. 2.1.4. Geosci. Model Dev. 8, 1991–2007. doi:10.5194/gmd-8-1991-2015

Costanzo, D., Cappadonia, C., Conoscenti, C., Rotigliano, E., 2012. Exporting a Google Earth™ aided earth-flow susceptibility model: a test in central Sicily. Nat. Hazards 61, 103–114. doi:10.1007/s11069-011-9870-0

Cruden, D.M., Varnes, D.J., 1996. Landslide types and processes, in: Turner, A.K., Schuster, R.L. (Eds.), Landslides: Investiga- Tion and Mitigation. Transportation Research Board Special Report, Vol. 247. National Academy Press, Washington D.C., pp. 36–75.

Felicísimo, Á.M., Cuartero, A., Remondo, J., Quirós, E., 2013. Mapping landslide susceptibility with logistic regression, multiple adaptive regression splines, classification and regression trees, and maximum entropy methods: a comparative study. Landslides 10, 175–189. doi:10.1007/s10346-012-0320-1

Friedman, J.H., 1991. Multivariate adaptive regression splines. Ann. Stat. 19, 1–141.

Garosi, Y., Sheklabadi, M., Porghasemi, H.R., Besalatpour, A.A., Conoscenti, C., Van Oost, K., 2018. Comparison of differences in resolution and sources of controlling factors for gully erosion susceptibility mapping. Geoderma 330, 65–78. doi:10.1016/j.geoderma.2018.05.027

Goetz, J.N., Brenning, A., Petschko, H., Leopold, P., 2015. Evaluating machine learning and statistical prediction techniques for landslide susceptibility modeling. Comput. Geosci. 81, 1–11. doi:10.1016/j.cageo.2015.04.007

Gómez-Gutiérrez, Á., Conoscenti, C., Angileri, S.E., Rotigliano, E., Schnabel, S., 2015. Using topographical attributes to evaluate gully erosion proneness (susceptibility) in two mediterranean basins: advantages and limitations. Nat. Hazards 79, 291–314. doi:10.1007/s11069-015-1703-0

Gorum, T., Gonencgil, B., Gokceoglu, C., Nefeslioglu, H.A., 2008. Implementation of reconstructed geomorphologic units in landslide susceptibility mapping: the Melen Gorge (NW Turkey). Nat. Hazards 46, 323–351. doi:10.1007/s11069-007-9190-6

Guisan, A., Weiss, S.B., Weiss, A.D., 1999. GLM versus CCA spatial modeling of plant species distribution. Plant Ecol. 143, 107–122.

Guzzetti, F., Carrara, A., Cardinali, M., Reichenbach, P., 1999. Landslide hazard evaluation: a review of current techniques and their application in a multi-scale study, Central Italy. Geomorphology 31, 181–216. doi:10.1016/S0169-555X(99)00078-1

Heckmann, T., Gegg, K., Gegg, a., Becht, M., 2014. Sample size matters: investigating the effect of sample size on a logistic regression susceptibility model for debris flows. Nat. Hazards Earth Syst. Sci. 14, 259–278. doi:10.5194/nhess-14-259-2014

Hosmer, D.W., Lemeshow, S., 2000. Applied logistic regression, Wiley Series in Probability and Statistics, Wiley series in probability and statistics: Texts and references section. Wiley. doi:10.1198/tech.2002.s650

Hungr, O., Leroueil, S., Picarelli, L., 2014. The Varnes classification of landslide types, an update. Landslides 11, 167–194. doi:10.1007/s10346-013-0436-y

Jebur, M.N., Pradhan, B., Tehrany, M.S., 2014. Optimization of landslide conditioning factors using very high-resolution airborne laser scanning (LiDAR) data at catchment scale. Remote Sens. Environ. 152, 150–165. doi:10.1016/j.rse.2014.05.013

Köthe, R., Lehmeier, F., 1996. SARA - System zur Automatischen Relief-Analyse, Benutzerhandbuch. Department of Geography, University of Göttingen, Göttingen.

Larsen, M.C., Wieczorek, G.F., 2006. Geomorphic effects of large debris flows and flash floods, northern Venezuela, 1999. Zeitschrift fur Geomorphol. 145, 147–175.

Larsen, M.C., 2008. Rainfall-triggered landslides, anthropogenic hazards, and mitigation strategies. Adv. Geosci. 14, 147–153. doi:10.5194/adgeo-14-147-2008

Lóczy, D., Pirkhoffer, E., Gyenizse, P., 2012. Geomorphometric floodplain classification in a hill region of Hungary. Geomorphology 147–148, 61–72. doi:10.1016/j.geomorph.2011.06.040

Lombardo, L., Cama, M., Conoscenti, C., Märker, M., Rotigliano, E., 2015. Binary logistic regression versus stochastic gradient boosted decision trees in assessing landslide susceptibility for multiple-occurring landslide events: application to the 2009 storm event in Messina (Sicily, southern Italy). Nat. Hazards 79, 1621–1648. doi:10.1007/s11069-015-1915-3

Lombardo, L., Cama, M., Maerker, M., Rotigliano, E., 2014. A test of transferability for landslides susceptibility models under extreme climatic events: application to the Messina 2009 disaster. Nat. Hazards 1951–1989. doi:10.1007/s11069-014-1285-2

Mathew, J., Jha, V.K., Rawat, G.S., 2009. Landslide susceptibility zonation mapping and its validation in part of Garhwal Lesser Himalaya, India, using binary logistic regression analysis and receiver operating characteristic curve method. Landslides 6, 17–26. doi:10.1007/s10346-008-0138-z

Milborrow, S., 2015. Notes on the earth package [WWW Document]. URL http://www.milbo.org/doc/earth-notes.pdf (accessed 7.15.15).

Naimi, B., 2015. Uncertainty analysis for species distribution models. R Software Package.

Nefeslioglu, H.A., Gokceoglu, C., Sonmez, H., 2008. An assessment on the use of logistic regression and artificial neural networks with different sampling strategies for the preparation of landslide susceptibility maps. Eng. Geol. 97, 171–191. doi:10.1016/j.enggeo.2008.01.004

Nicu, I.C., Asăndulesei, A., 2018. GIS-based evaluation of diagnostic areas in landslide susceptibility analysis of Bahluieț River Basin (Moldavian Plateau, NE Romania). Are Neolithic sites in danger? Geomorphology 314, 27–41. doi:10.1016/j.geomorph.2018.04.010

Ohlmacher, G.C., 2007. Plan curvature and landslide probability in regions dominated by earth flows and earth slides. Eng. Geol. 91, 117–134. doi:10.1016/j.enggeo.2007.01.005

Pourghasemi, H.R., Rossi, M., 2016. Landslide susceptibility modeling in a landslide prone area in Mazandarn Province, north of Iran: a comparison between GLM, GAM, MARS, and M-AHP methods. Theor. Appl. Climatol. doi:10.1007/s00704-016-1919-2

R Core Team, 2017. R: A Language and Environment for Statistical Computing.

Regmi, N.R., Giardino, J.R., McDonald, E. V., Vitek, J.D., 2014. A comparison of logistic regression-based models of susceptibility to landslides in western Colorado, USA. Landslides 11, 247–262. doi:10.1007/s10346-012-0380-2

Reichenbach, P., Rossi, M., Malamud, B.D., Mihir, M., Guzzetti, F., 2018. A review of statistically-based landslide susceptibility models. Earth-Science Rev. 180, 60–91. doi:10.1016/j.earscirev.2018.03.001

Rotigliano, E., Agnesi, V., Cappadonia, C., Conoscenti, C., 2011. The role of the diagnostic areas in the assessment of landslide susceptibility models: a test in the sicilian chain. Nat. Hazards 58, 981–999. doi:10.1007/s11069-010-9708-1

Rotigliano, E., Martinello, C., Agnesi, V., Conoscenti, C., 2018. Evaluation of debris flow susceptibility in El Salvador (CA): a comparison between Multivariate Adaptive Regression Splines (MARS) and Binary Logistic Regression (BLR). Hungarian Geogr. Bull. 67, 361–373. doi:10.15201/hungeobull.67.4.5

Ruß, G., Brenning, A., 2010. Computational Intelligence for Knowledge-Based Systems Design, Lecture Notes in Computer Science (including subseries Lecture Notes in Artificial Intelligence and Lecture Notes in Bioinformatics), Lecture Notes in Computer Science. Springer Berlin Heidelberg, Berlin, Heidelberg. doi:10.1007/978-3-642-14049-5

Süzen, M.L., Doyuran, V., 2004. Data driven bivariate landslide susceptibility assessment using geographical information systems: a method and application to Asarsuyu catchment, Turkey. Eng. Geol. 71, 303–321. doi:10.1016/S0013-7952(03)00143-1

Svoray, T., Michailov, E., Cohen, A., Rokah, L., Sturm, A., 2012. Predicting gully initiation: comparing data mining techniques, analytical hierarchy processes and the topographic threshold. Earth Surf. Process. Landforms 37, 607–619. doi:10.1002/esp.2273

Trigila, A., Iadanza, C., Esposito, C., Scarascia-Mugnozza, G., 2015. Comparison of Logistic Regression and Random Forests techniques for shallow landslide susceptibility assessment in Giampilieri (NE Sicily, Italy). Geomorphology. https://doi.org/10.1016/j.geomorph.2015.06.001

Van Den Eeckhaut, M., Hervás, J., Jaedicke, C., Malet, J.P., Montanarella, L., Nadim, F., 2012. Statistical modelling of Europe-wide landslide susceptibility using limited landslide inventory data. Landslides 9, 357–369. doi:10.1007/s10346-011-0299-z

Van Den Eeckhaut, M., Vanwalleghem, T., Poesen, J., Govers, G., Verstraeten, G., Vandekerckhove, L., 2006. Prediction of landslide susceptibility using rare events logistic regression: A case-study in the Flemish Ardennes (Belgium). Geomorphology 76, 392–410. doi:10.1016/j.geomorph.2005.12.003

Vorpahl, P., Elsenbeer, H., Märker, M., Schröder, B., 2012. How can statistical models help to determine driving factors of landslides? Ecol. Modell. 239, 27–39. doi:10.1016/j.ecolmodel.2011.12.007

Wilson, J.P., Gallant, J.C., 2000. Terrain Analysis: Principles and Apllications. Wiley & Sons, Inc., Canada.

Zevenbergen, L.W., Thorne, C.R., 1987. Quantitative analysis of land surface topography. Earth Surf. Process. Landforms 12, 47–56.

Figure 1 (Color)
Click here to download high resolution image

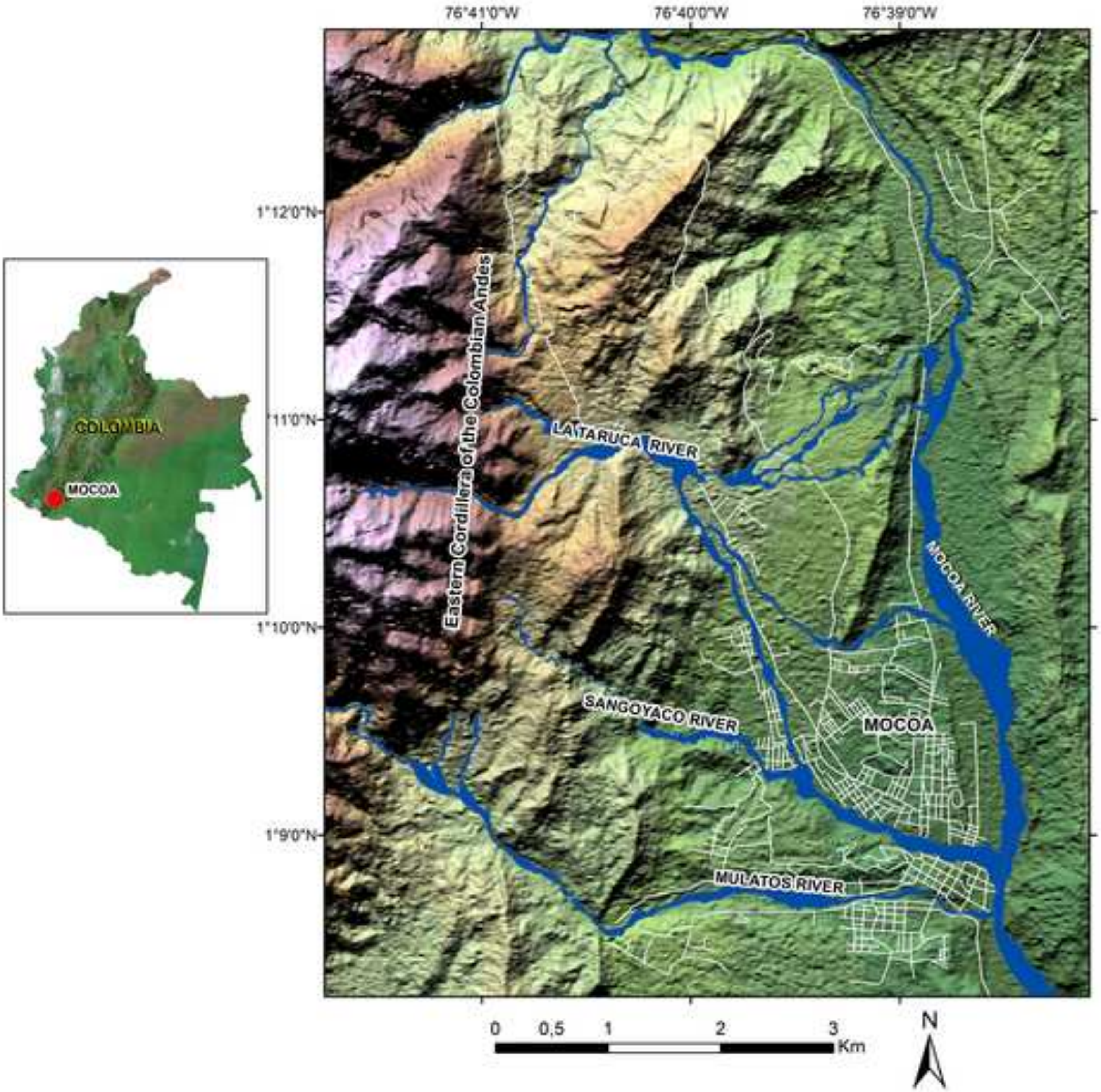

Figure (Color)
Click here to download high resolution image

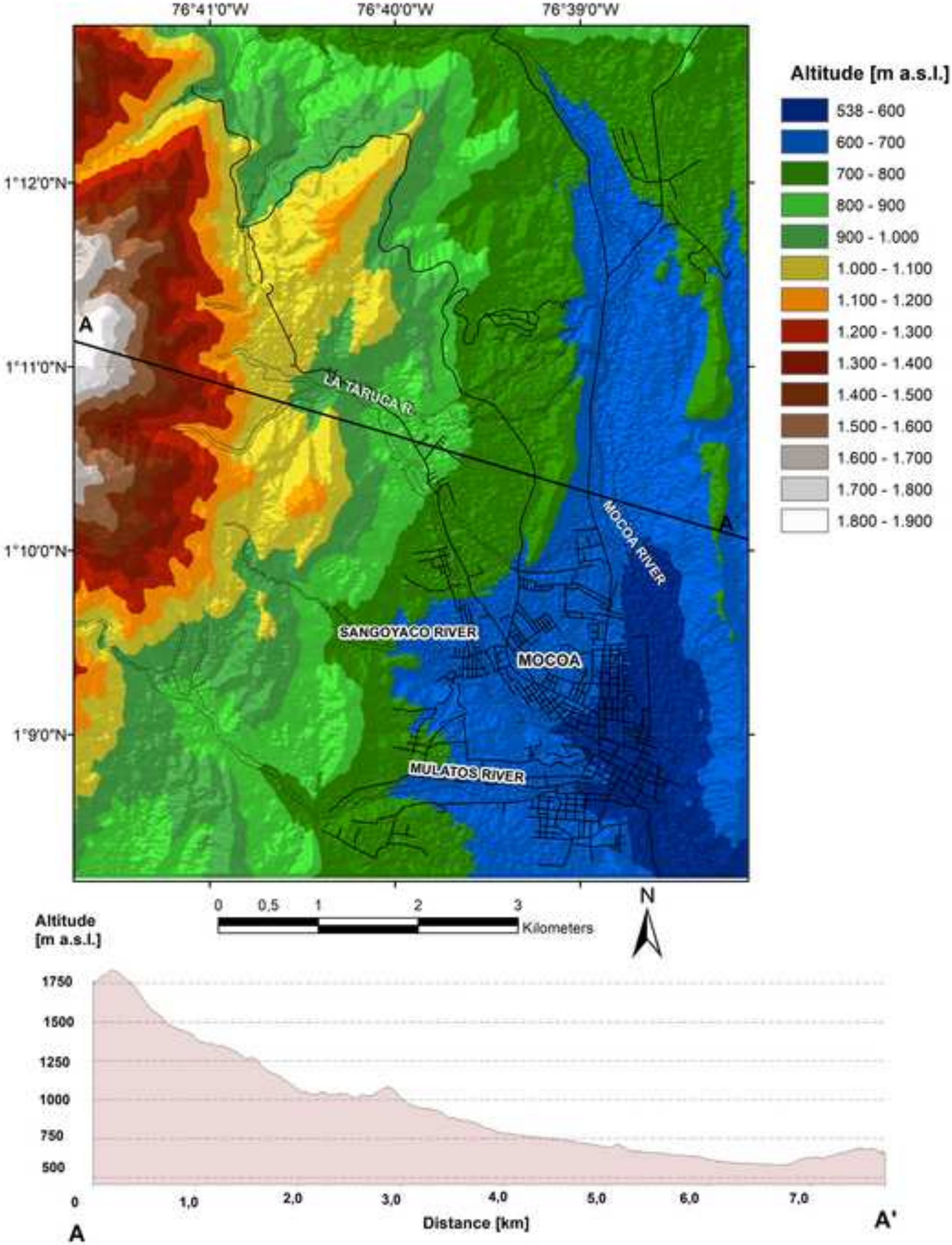

Figure (Color)
Click here to download high resolution image

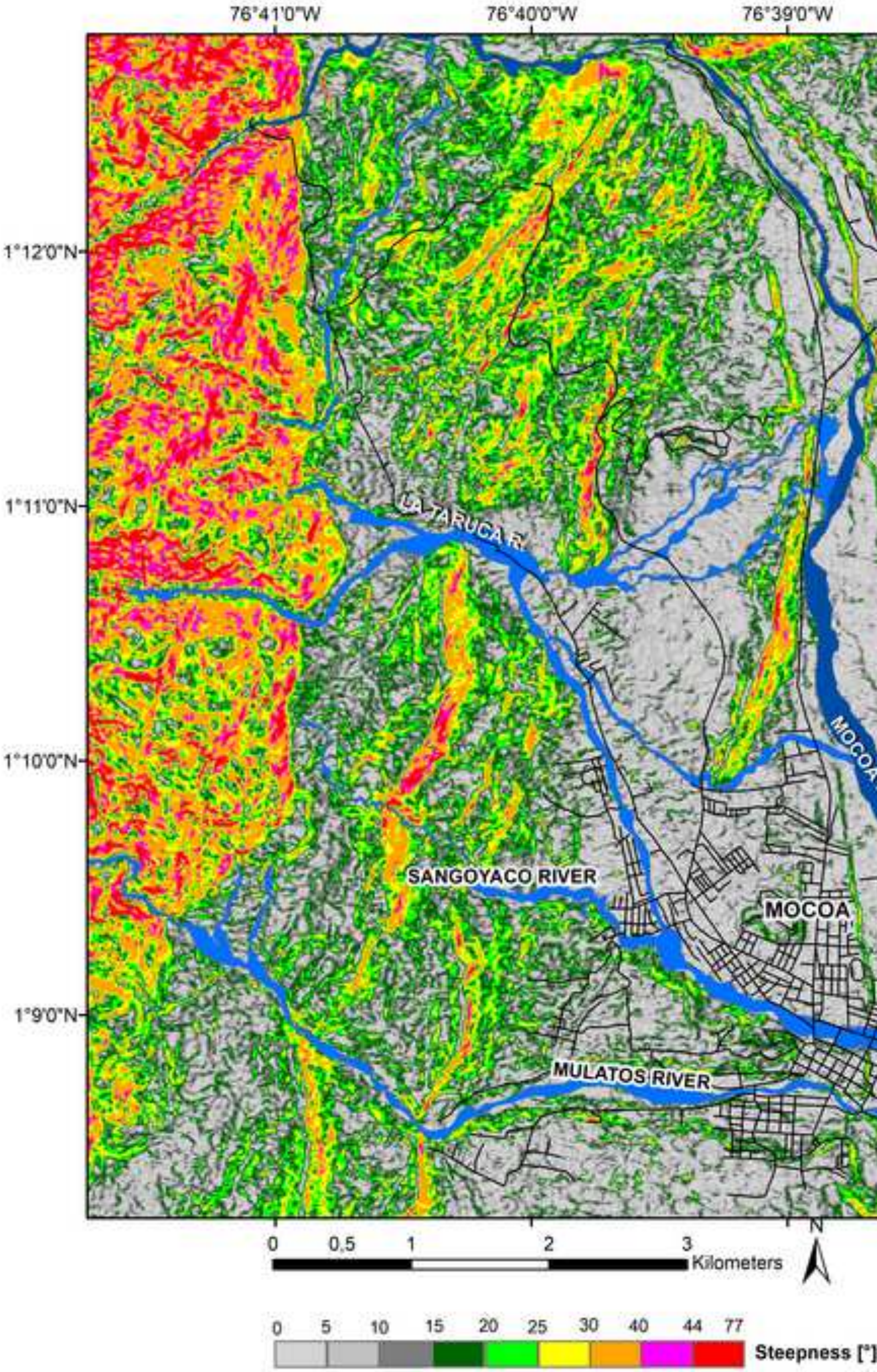

Figure (Color)
Click here to download high resolution image

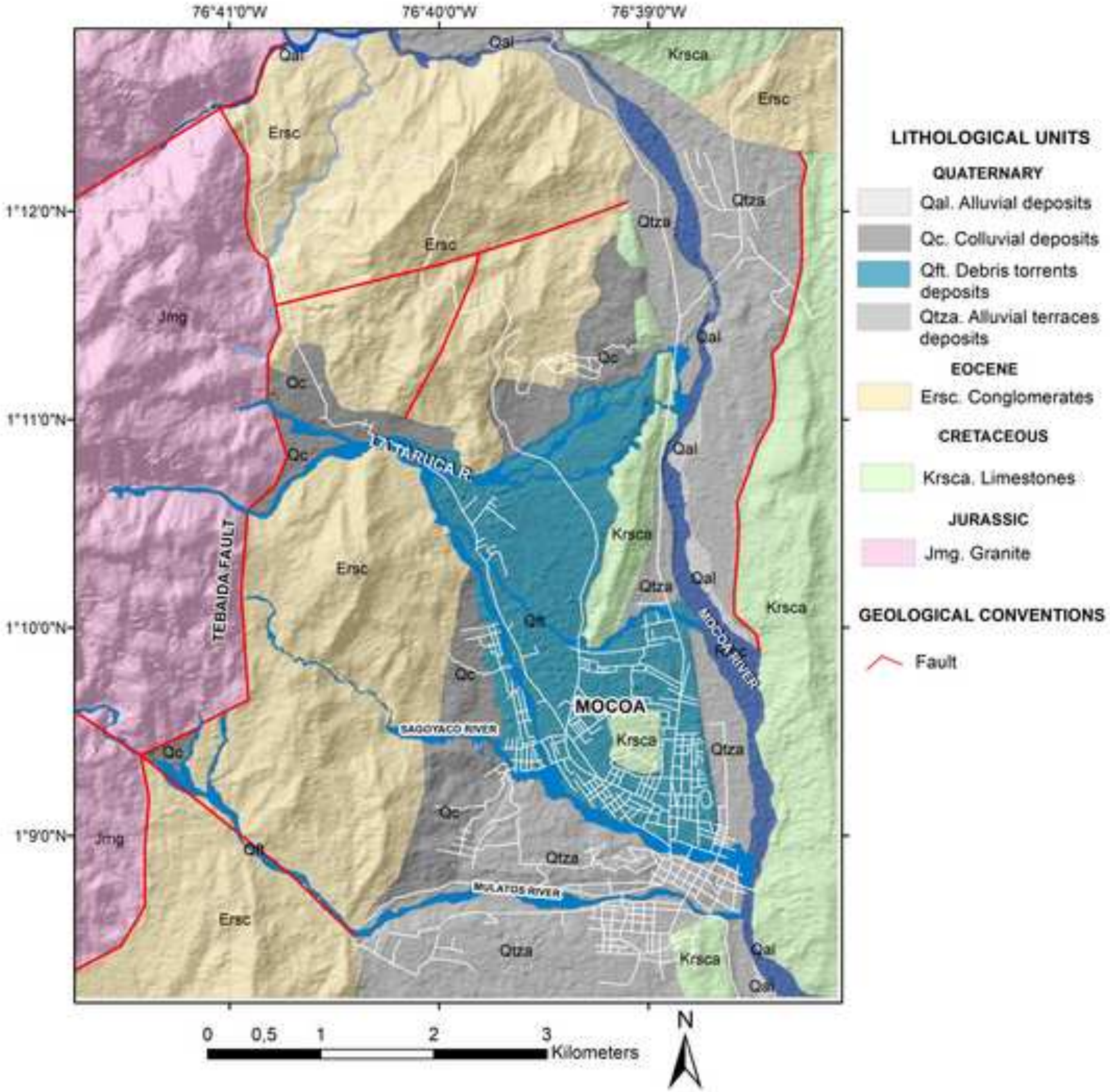

Figure (Color)
Click here to download high resolution image

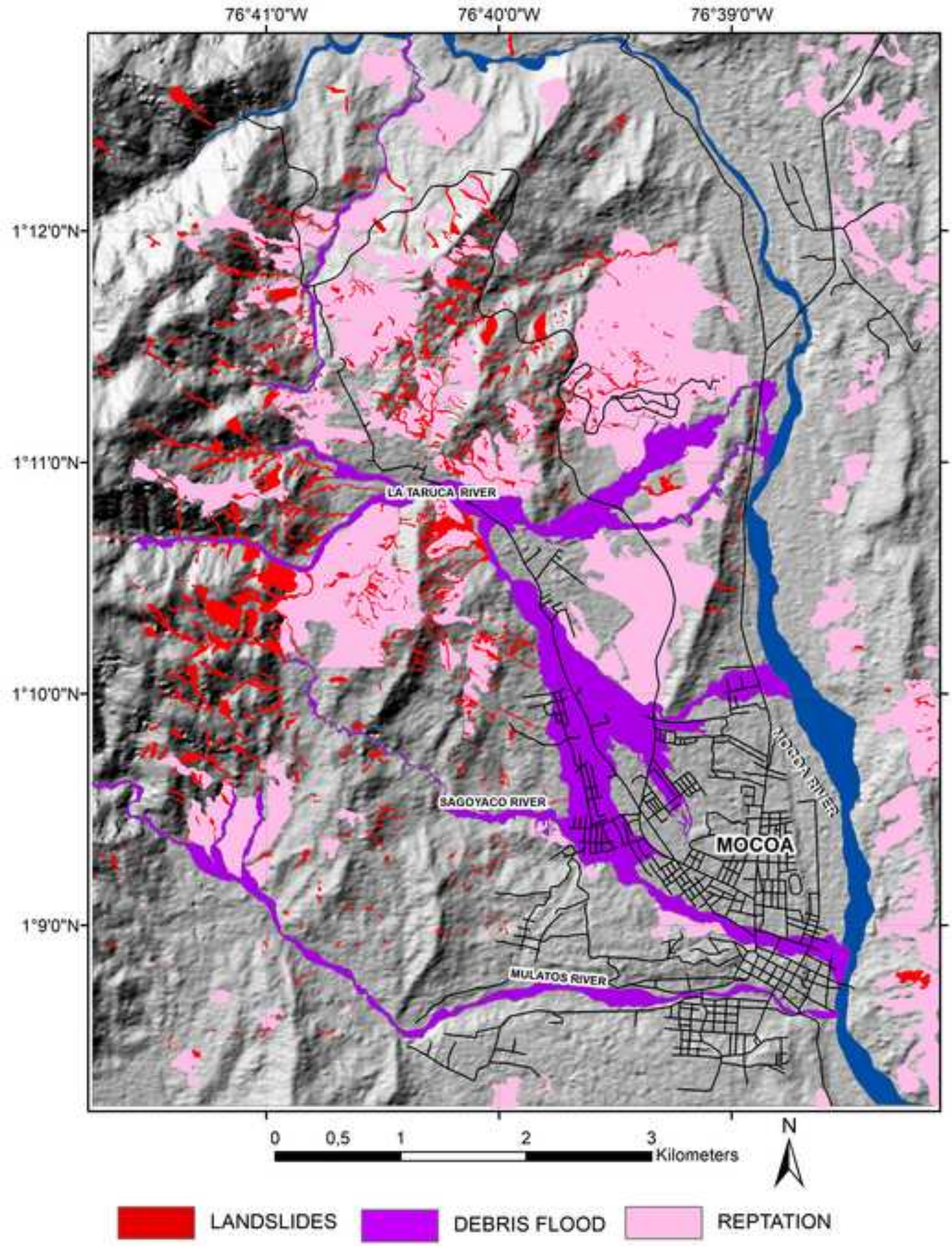

Figure (Color)
Click here to download high resolution image

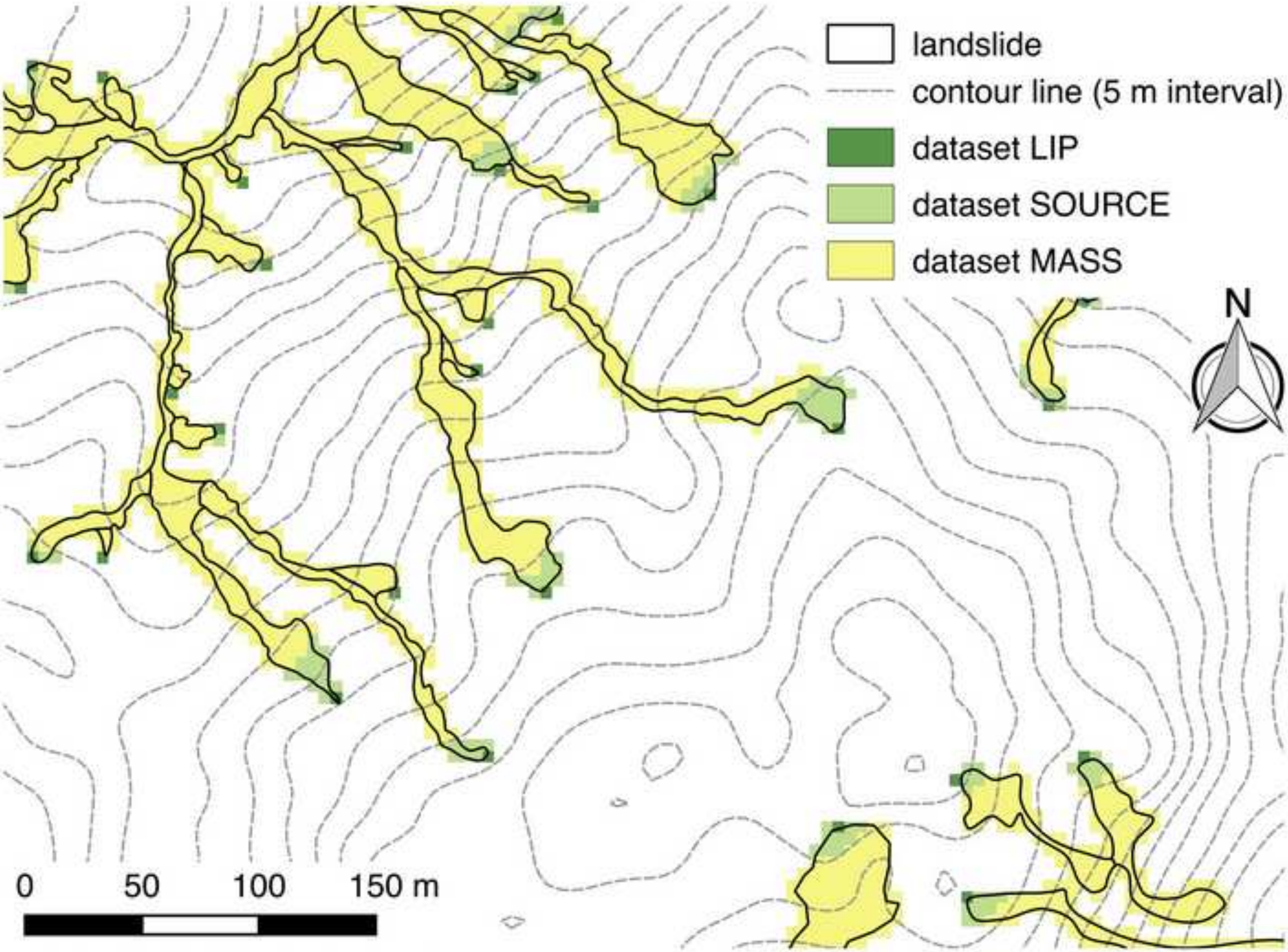

Figure (Color)
Click here to download high resolution image

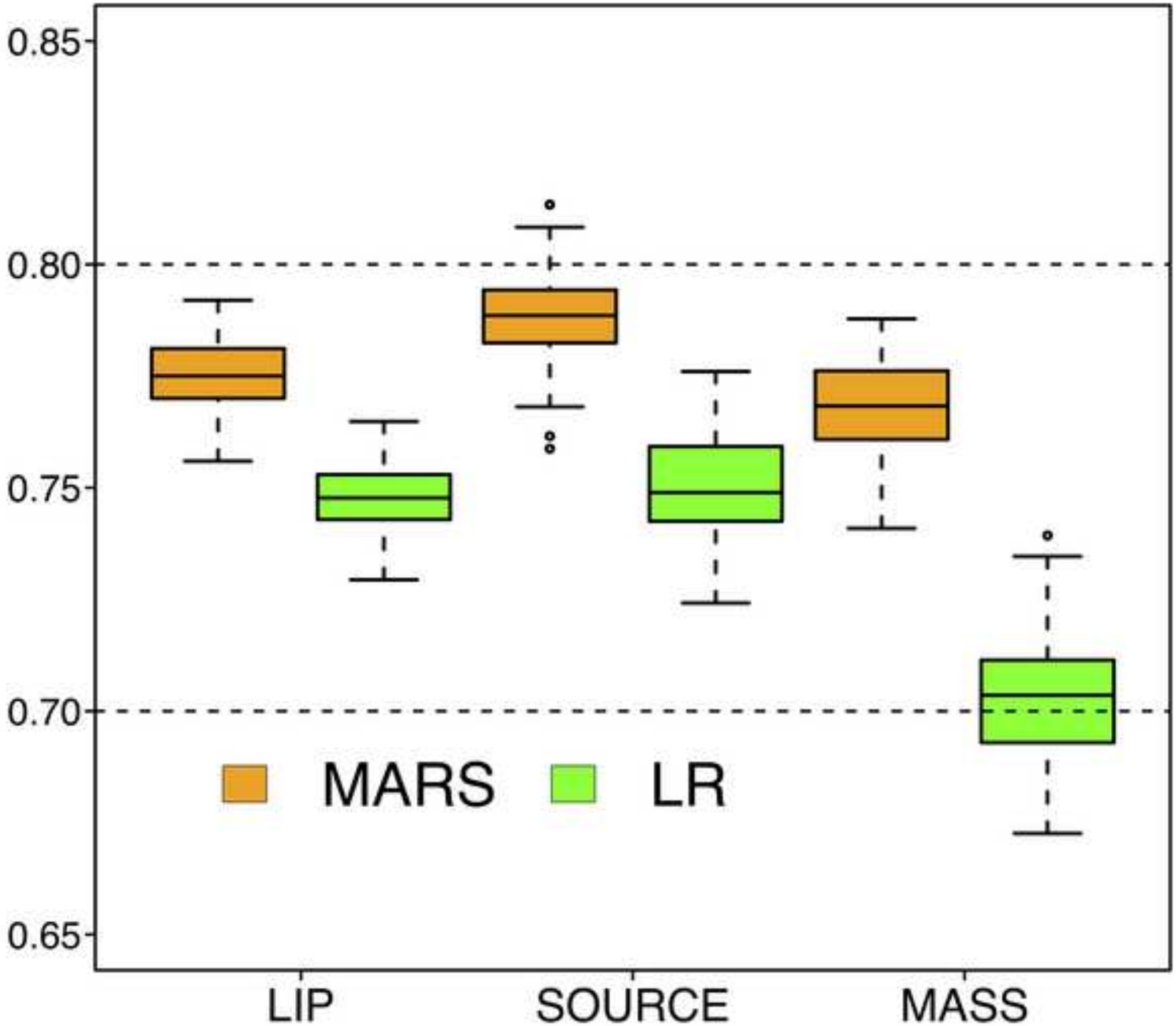

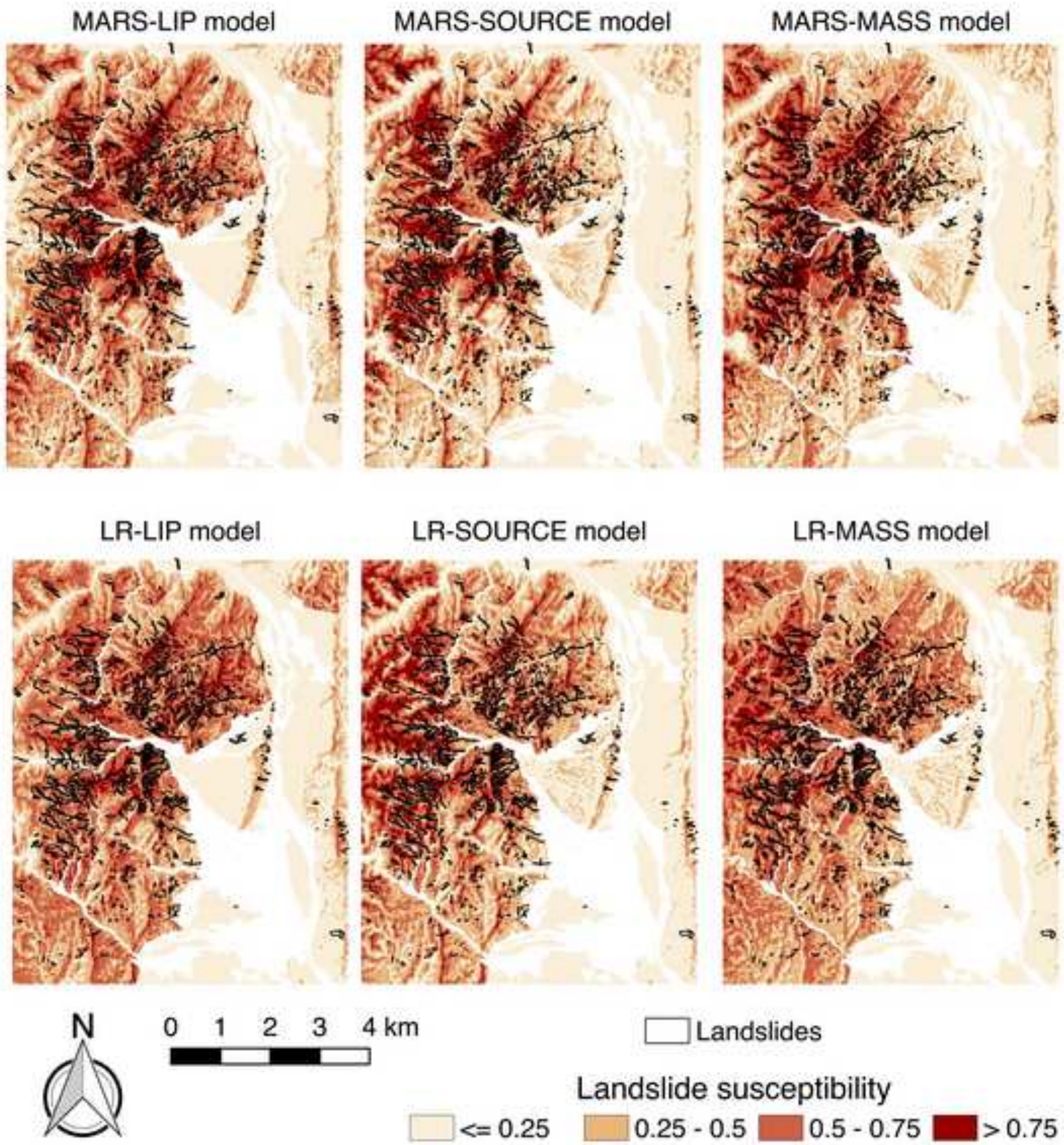
MARS-LIP model
MARS-SOURCE model
MARS-MASS model
LR-LIP model
LR-SOURCE model
LR-MASS model
N
0 1 2 3 4 km
Landslides
Landslide susceptibility
<= 0.25
0.25 - 0.5
0.5 - 0.75
> 0.75

Figure (Color)
Click here to download high resolution image